Hydro dB

Hydro dB, LLC

Seattle, Washington

Modeling of Sound Propagation from Pile Driving Marine Construction at Seal Beach
Peter H. Dahl, Ph.D.

21 October 2018

This report summarizes the modeling of the underwater sound field from pile driving associated with naval marine construction activity at Seal Beach and the entrance to Anaheim Bay. Section I outlines the modeling methods and Section II provides some representative results. Final results have been provided to Tierra Data Inc. (Jim Kellogg) for implementation into spatial maps to be used estimation of potential marine mammal zone of impact. (Note: this report includes a revision to the original dated 14 October, relating to Figs. 3 and 4.)

Section I: Modeling methods

The propagation model is developed for transmission loss (TL) applies to both impact and vibratory pile driving at given pile location, as currently there does not exist empirical evidence to justify two separate propagation models. Four pile locations are assessed. The first (site 1) is a single representative central location associated with construction of the new ammunition pier at Seal Beach. This is the key pile location associated with marine construction. In addition, three addition sites representing installation of the two Oscar buoys (sites 2 and 3) located outside the breakwater, and a representative central location for the installation of the three Echo buoys (site 3) that are located inside the breakwater; these buoys are not sufficiently separated to justify separate locations for evaluation.

In the propagation model the pile is represented as a uniform line source of sound [1-3] extending over the depth of the water column corresponding to the water depth at the pile driving location. Sources of sound are distributed every 0.5 m, starting at depth 0.5 m and extending to the bottom.

The water depth corresponds to a mean sea level (MSL), based on the bathymetry and structural feature data received from Tierra Data Inc. There is some tidal variation in this depth, however, we believe the basic trends in prediction are captured through use of the MSL depth.

For each source at depth z_i, and for a particular acoustic frequency, f, (as discussed given below) adiabatic mode theory [4] is used to compute the acoustic pressure field as a function of range, r, and receiver depth, z. For modeling purposes we characterize the seabed using typical values for sand: sound speed of 1650 m/s, sediment density equal to 1.2 times the density of seawater, and sediment attenuation of 0.3 dB/m/kHz.

Computation is undertaken for every transect, or radial, that radiates away from the pile source location in increments of 1°. The computation is then repeated using a different source depth, with results from all source depths incoherently summed (i.e., summing the magnitude square of each source at depth z_i,).

Thus, for a given acoustic frequency we derive a field quantity p that is a function of range and depth, or $|p_n(r,z;f)|^2$ where the subscript n denotes the particular radial.

The computations are made at six frequencies corresponding to octave-band center frequencies: 63 Hz, 125 Hz, 250 Hz, 500 Hz, 1000 Hz and 2000 Hz. These frequencies represent the key octave band center frequencies associated with both impact and vibratory pile driving. (This does not imply the upper range of sound is limited to 2000 Hz. Instead it is this spread of frequencies, 63-2000 Hz, which is used to model propagation physics.)

The results for $|p_n(r,z;f)|^2$ at six frequencies generated at each of the four sites are now weighted by a normalized pressure spectral density, $S(f)$, representing an average, normalized pressure spectral densities for both vibratory and impact pile driving that depends on pile type. The three piles types are:

(1) 30 inch diameter steel pile
(2) 24 inch cement pile
(3) 14 inch H (or I) type pile

Values for $S(f)$ need to be generated through empirical means. For the 30 inch steel piles we use the spectrum from [1] to generate $S(f)$, and for the other two pile types we use spectra from California Dept. of Transportation report [5]. The results for the three pile types are summarized in Table 1

Center Frequency (Hz)	Bandwidth (Hz)	$S(f)$ 30 inch Steel [1]	$S(f)$ 24 inch cement [5]	$S(f)$ H/I type [5]
63	44	0.63	1.0	0.32
125	89	0.85	0.30	1.0
250	178	1.0	0.06	0.97
500	355	0.53	0.04	0.90
1000	710	0.19	0.001	0.18
2000	1420	0.06	0.001	0.07

Table 1. Normalized Pressure Spectral Density spectral strengths and bandwidths.

The $S(f)$ function is then used to weight the stored $|p_n(r,z;f)|^2$ computations corresponding to each of the six center frequencies in Table 1. For example, for 30 inch steel piles, $|p_n(r,z;f)|^2$ for f = 250 Hz (the spectral peak) is given a weight (spectral strength) of 1, whereas for f = 2000 Hz this weight is 0.06. Thus at 250 Hz the contribution to mean-square pressure is: $|p_n(r,z;f)|^2$ * (1) *178, the value 1 coming from $S(f)$ at 250 Hz and the value 178 associated with the octave bandwidth, B (f), at 250 Hz (Table 1). This is completed for each of the six frequencies for a given pile type (representing an implementation of Parseval's theorem.)

For each $|p_n(r,z;f)|^2$ * $S(f)$ * B(f) at a given radial separated in increments of 1° we undertake an average over depth (where depth will vary with range according to the particular radial).

The depth-average result is now a function only of range r and frequency f which we call $I_n(r;f)$. We must ultimately sum the $I_n(r;f)$ over the six frequencies, but not until a barrier diffraction correction is applied which is discussed next.

Shadowing and diffraction of sound by the new breakwater feature (Fig. 1) will occur for pile locations associated with the new ammunition pier, and the Echo buoys. In Fig. 1, radials associated with pile driving for the ammunition pier are shown radiating at 1^o increments. For any radial that is shadowed by the new breakwater, represented by all radials within the two red lines, strong shadowing by the breakwater will occur

Our approach to modeling this effect is to allow sound to emerge on the outside of the barrier based on some recent work on the diffraction of underwater sound by barriers [6]. The essence of this approach is to compute the path difference (Fig. 2) between a radial that intersects the barrier (path A) and a path that must first reach the edge of the barrier before turning inward (path B). The difference in path lengths, divided by the ½ the acoustic wavelength, is known as the Fresnel number. For large Fresnel numbers (high frequencies) the barrier shadowing is strong whereas for smaller Fresnel numbers (lower frequencies) the shadowing is weaker but still significant. In Ref. [6] an empirical formulation is given that predicts the reduction in sound level as function of Fresnel number which is used here. Applying the basic geometry shown in Fig. 1, we compute this reduction as fractional reduction in intensity as function range and frequency for all radials n that intersect the barrier.

Let us call this quantity $D_n(r,f)$. For example, a radial directed outwards and into the entrance of Anaheim Bay (Fig. 1) will have $D_n(r,f)$ equal to 1, or a 0 dB reduction, until it intersects the barrier after which $D_n(r,f)$ will be less than 1 and vary with distance from the barrier and frequency. Values for $D_n(r,f)$ will be typically quite small, i.e., << 1, representing a large fractional reduction in intensity and subsequent shadowing as a result of the barrier.

We also compute $D_n(r,f)$ for the other 3 pile locations representing the two Oscar buoy locations and the centroidal Echo buoy location, and the two yellow squares in Fig. 1 represent locations where additional shadowing loss is computed using the path-difference formulation.

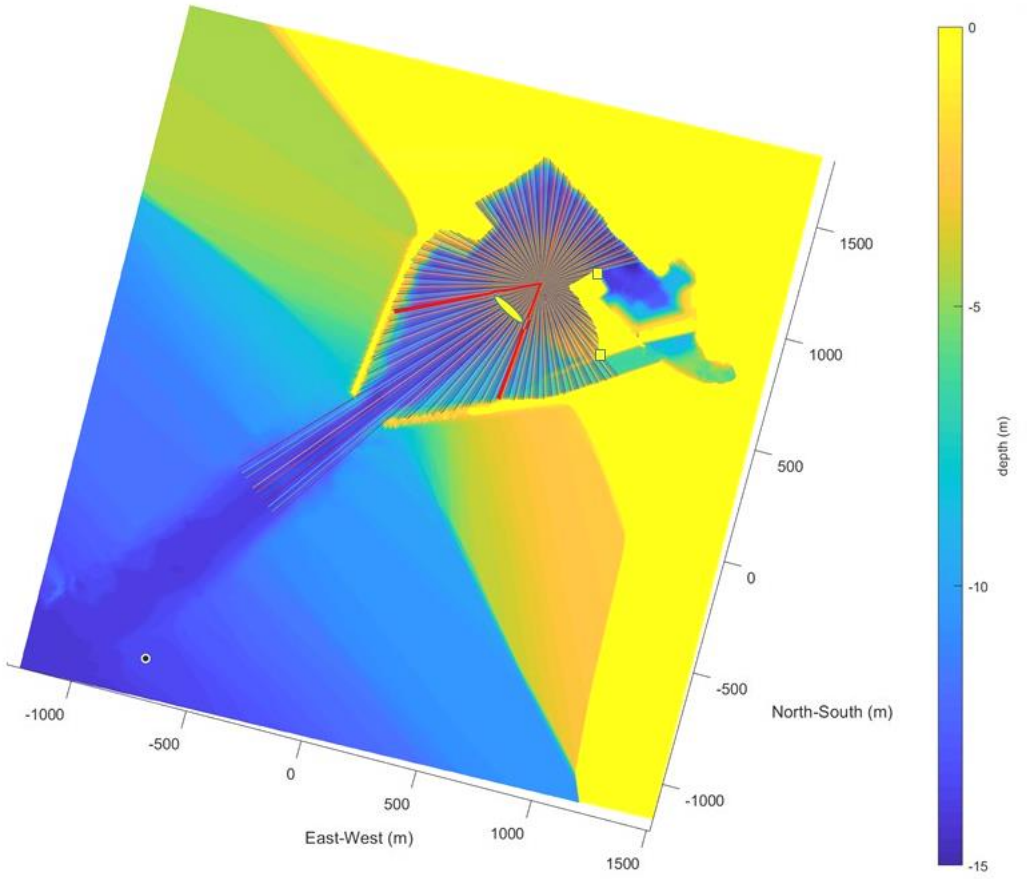

Fig. 1 Inner bay construction region showing transects radiating at increments of 1° from the pile location for construction of the new ammunition pier. The new breakwater is symbolized by the yellow feature in the center of the map. Two radials that intersect the edge of the breakwater are shown in red and all radials between these two are influenced by the breakwater. The two small yellow squares also represent diffraction edges discussed in text.

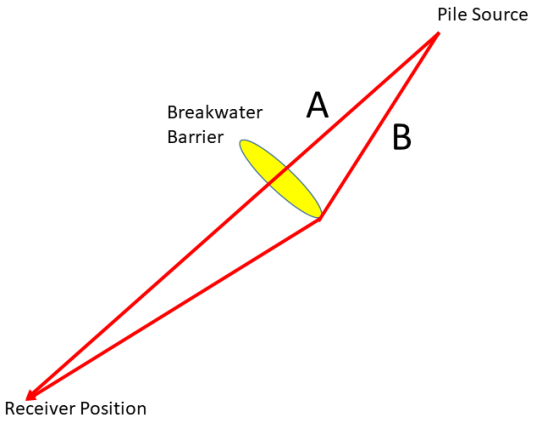

Fig. 2 Diagram showing two paths: A which intersects the barrier and B which strikes the edge of the barrier. The Fresnel number for the receiver position is computed on the basis of the difference in the two path lengths.

The next step is to multiply each $I_n(r;f)$ by the corresponding $D_n(r,f)$and then a sum over the six frequencies, calling the new quantity $I_n(r)$. The final step is to express $I_n(r)$ in decibels and reference it to a range of 10 m, such that transmission loss for given radial, $TL_n(r)$, equals 0 dB at range 10 m.

This is done as follows:

$TL_n(r) = 10 \log10 [I_n(r)/ I_n(r= 10 \text{ m})]$

Pile Data source Data referenced to range 10 m	30 inch steel San Diego Fuel Pier supplied by Tierra Data	24 inch concrete Table 2.2 Ref. [5]	I/H beam Fig. I.4-8, Ref. [5]
Peak dB re μPa	216	193	194
RMS dB re μPa	201	175	181
SEL dB re μPa^2 sec	185	160	171
Vibratory RMS dB re μPa	170	No data	170 (as per email Todd McConchie, Tierra Data Inc. 10-16-18)

Table 2. Pile source strength data as would be measured at range 10 m.

Examples representing pile driving associated with the ammunition pier site are shown next. The first set (Fig. 3) shows the model for the single strike SEL field associated with installation of a 30-inch steel pile. To compute SEL, the constant 185 (Table 2) is added to each 10-m referenced transmission loss, $TL_n(r)$. The second (Fig. 4) shows the model for the single strike SEL field associated with installation of a 24-inch cement pile. To compute SEL in this case the constant 160 (Table 2) is added.

The ammunition pier central pile location (white dot) is interior to the breakwater (see Fig. 1). The influence of the breakwater can be seen by the strong shadowing or reduction of SEL on the seaward side of the breakwater. It is possible that actual physical shadowing transition could be smoother than that conveyed here. However, we emphasize that accounting for the barrier diffraction is very difficult problem in underwater acoustic modeling. Our approach is innovative insofar as incorporating the results of the Japanese study [6], but it is also conservative. For example, one common approach to addressing this issue is to assume shadowing is complete and that *no sound* emerges on the outside of the barrier [7].

As rough qualitative guide, for the case of 30 inch steel piles (Fig 3) a single-strike SEL is expected to be about 120 re μPa^2 sec at the opening to Anaheim Bay. Assuming a maximum of 2000 strikes for a day, then the cumulative SEL will be about 153 dB. For the case of 24 inch cement piles (Fig. 4) the equivalent cumulative SEL will be considerably less. However, a more quantitative spatial description of the zones of influence will be provided in the mapping results subsequently generated at Tierra Data.

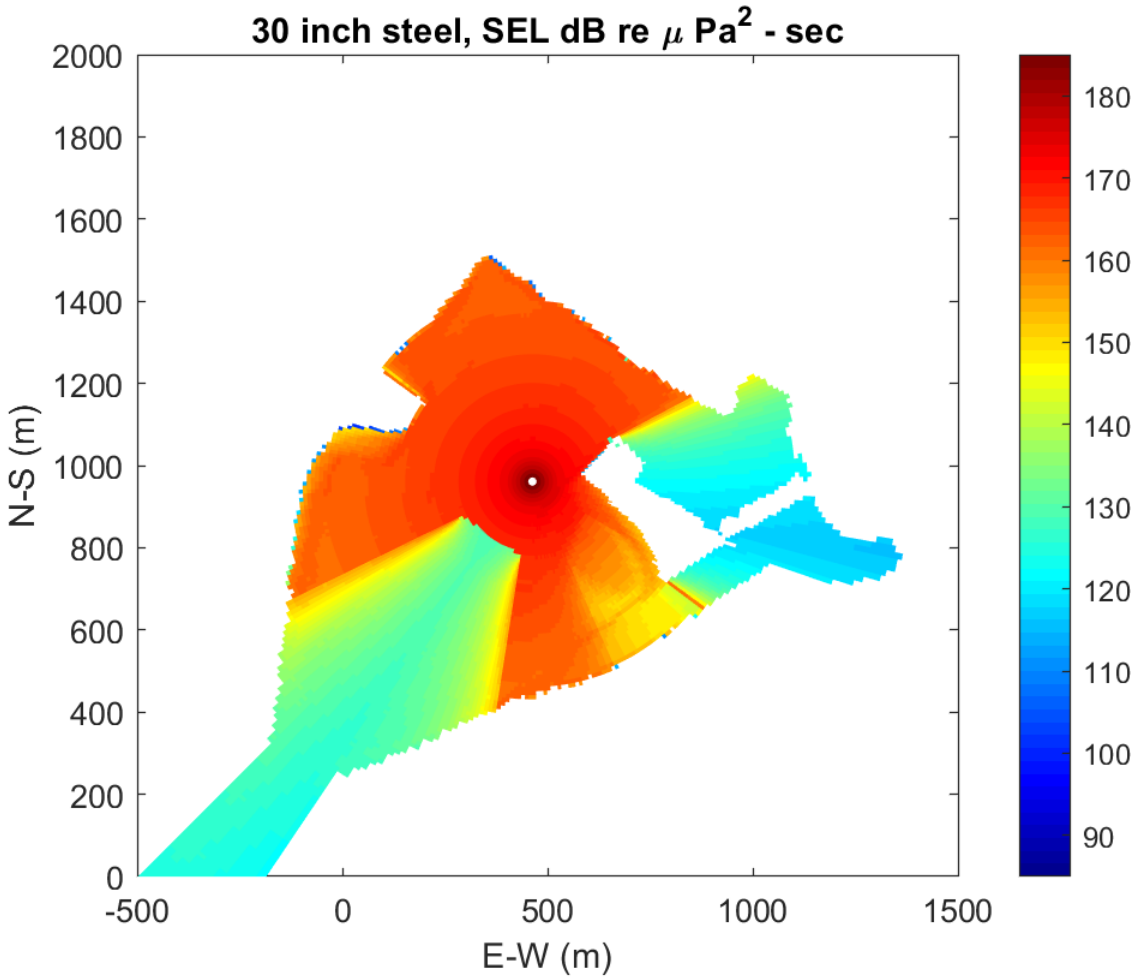

Fig. 3 Estimated single strike SEL for a 30 inch steel pile installed at the ammunition pier central location.

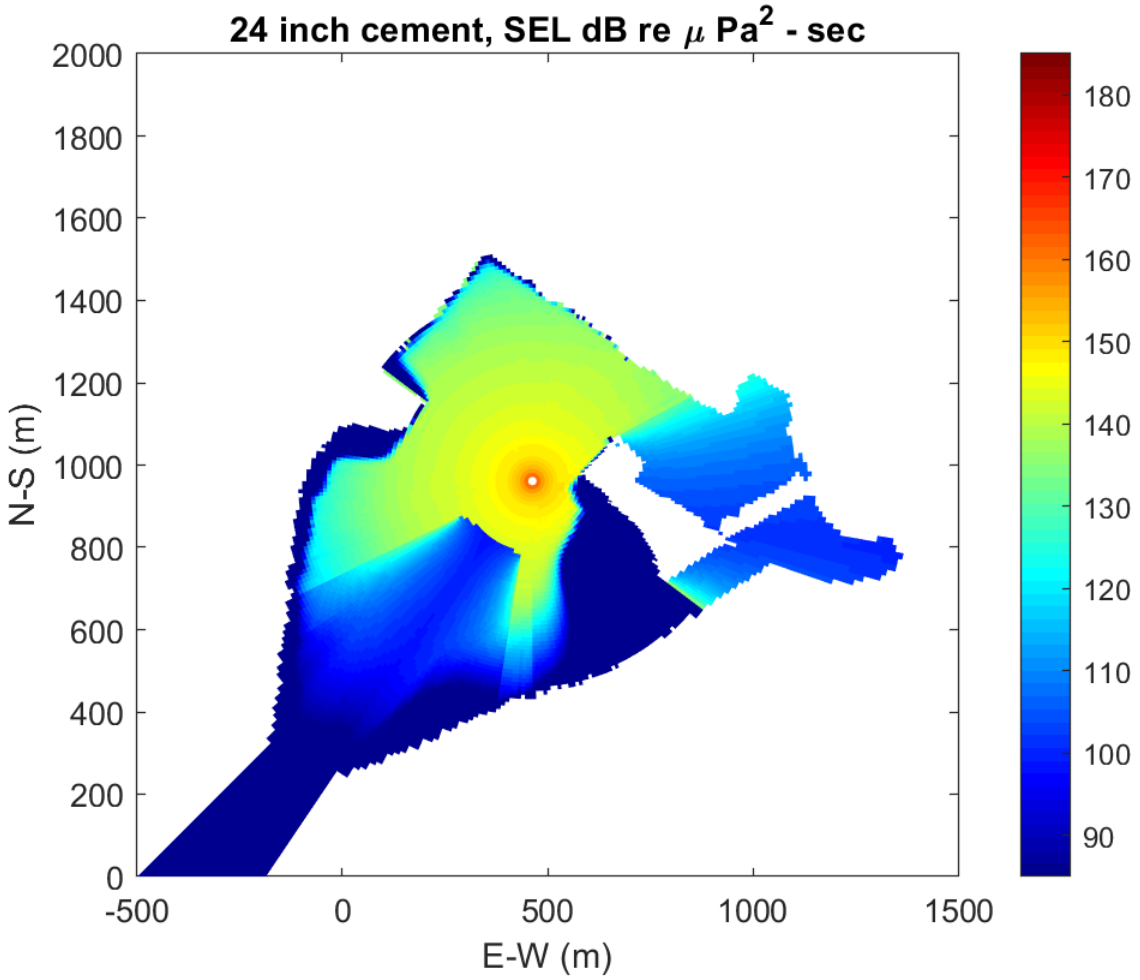

Fig. 4 Estimated single strike SEL for a 24 inch cement pile installed at the ammunition pier central location.

References

1. P.G. Reinhall, & P.H. Dahl, "Underwater Mach wave radiation from impact pile driving: Theory and observation", J. Acoust. Soc. Am. 130, 3, 1209-1216 (September 01, 2011).

2. P. H. Dahl, D.R. Dall'Osto and D.M. Farrell, "The underwater sound field from vibratory pile driving," J. Acoust. Soc. Am., 136, 3544-3554, June 2015.

3. P. H. Dahl and D.R. Dall'Osto, "On the underwater sound field from impact pile driving: Arrival structure, precursor arrivals, and energy streamlines", J. Acoust. Soc. Am., 142, 1141-1155, Aug. 2017.

4. C.T. Tindle and Z.Y. Zang, "An adiabatic normal mode solution for the benchmark wedge", J. Acoust. Soc. Am., 101, pp. 606-609, 1997

5. California Department of Transportation, "Technical Guidance for the Assessment and Mitigation for the Hydroacoustic Effects of Pile-driving on Fish" (2015), CalTrans Report Number: CTHWANP-RT-15-306.01.01

6. K. Kuramoto, S. Yamaguchi, K. Oimatsu, and S. Kuwahara, "Sound attenuation by barriers in underwater", J. Acoust. Soc. Jpn. (E) 15, 1 (1994)

7. Washington Dept. of Transportation (WSDOT) Biological Assessment Preparation Advanced Training Manual, 2013. Available online at: http://www.wsdot.wa.gov/environment/biology/ba/baguidance.htm